

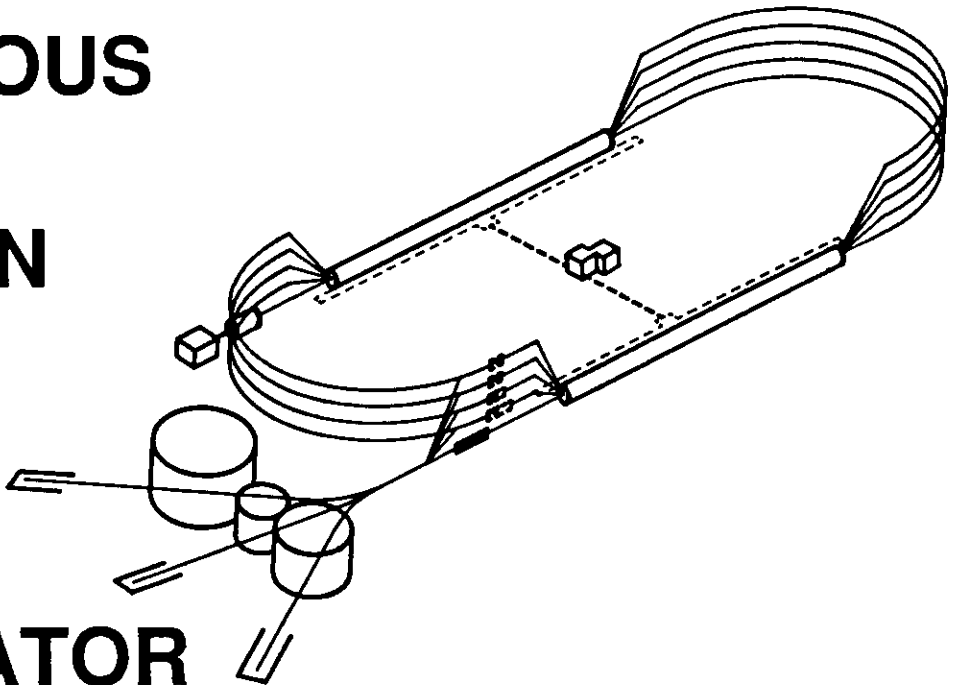
CEBAF PR-90-023  
October 1990

## Electronic Systems for Beam Position Monitors at CEBAF

*W. Barry, J. Heefner, J. Perry*  
*Continuous Electron Beam Accelerator Facility*  
*12000 Jefferson Avenue*  
*Newport News, VA 23606*

# C E B A F

CONTINUOUS  
ELECTRON  
BEAM  
ACCELERATOR  
FACILITY



**SURA** *Southeastern Universities Research Association*

**CEBAF**

The Continuous Electron Beam Accelerator Facility

Newport News, Virginia

Copies available from:

Library  
CEBAF  
12000 Jefferson Avenue  
Newport News  
Virginia 23606

The Southeastern Universities Research Association (SURA) operates the Continuous Electron Beam Accelerator Facility for the United States Department of Energy under contract DE-AC05-84ER40150.

#### DISCLAIMER

This report was prepared as an account of work sponsored by the United States government. Neither the United States nor the United States Department of Energy, nor any of their employees, makes any warranty, express or implied, or assumes any legal liability or responsibility for the accuracy, completeness, or usefulness of any information, apparatus, product, or process disclosed, or represents that its use would not infringe privately owned rights. Reference herein to any specific commercial product, process, or service by trade name, mark, manufacturer, or otherwise, does not necessarily constitute or imply its endorsement, recommendation, or favoring by the United States government or any agency thereof. The views and opinions of authors expressed herein do not necessarily state or reflect those of the United States government or any agency thereof.

2

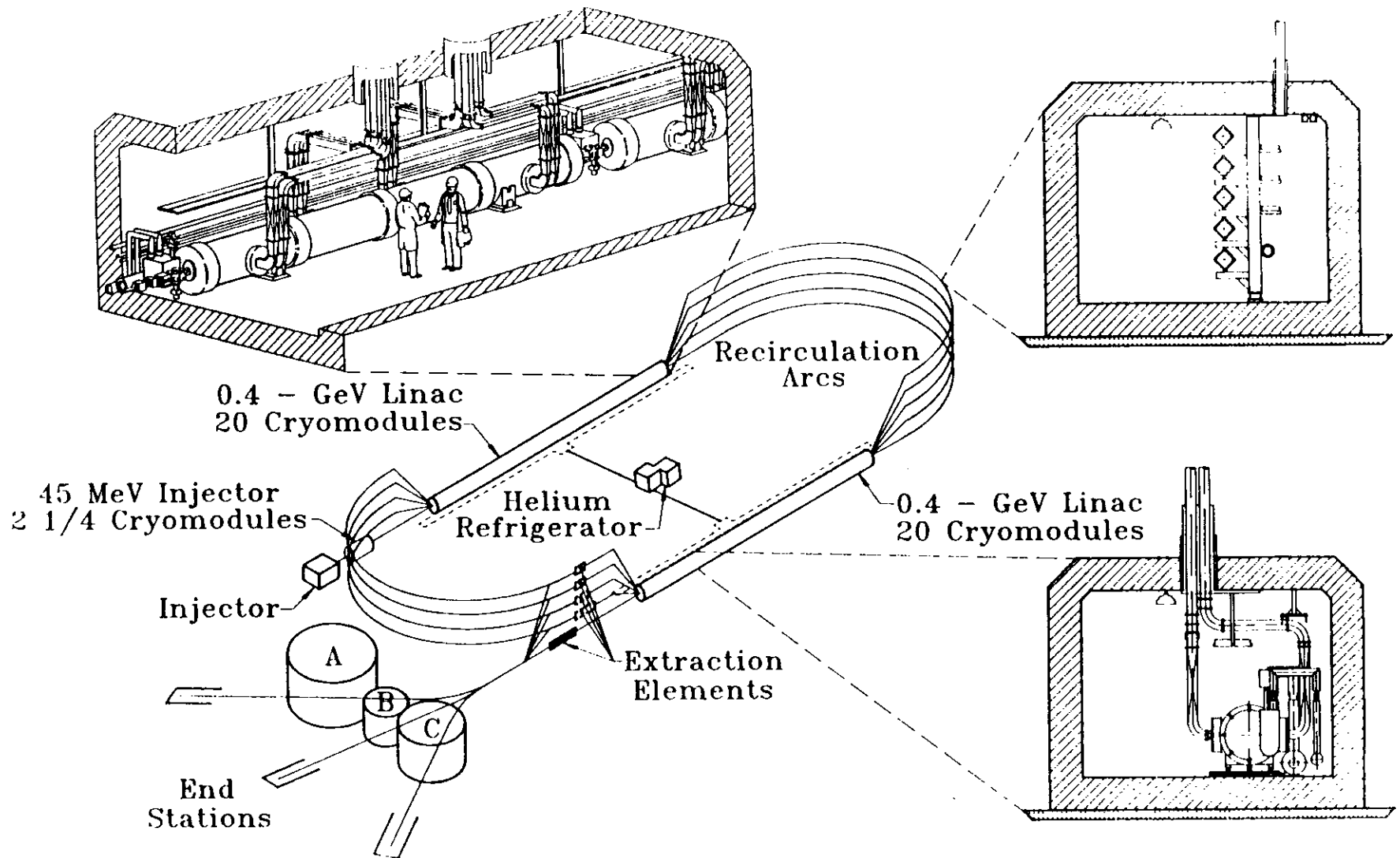


Figure 1. CEBAF machine configuration.

# ELECTRONIC SYSTEMS FOR BEAM POSITION MONITORS AT CEBAF\*

W. Barry, J. Heefner (presenter), and J. Perry  
Continuous Electron Beam Accelerator Facility  
12000 Jefferson Avenue, Newport News, VA 23606

## ABSTRACT

The Continuous Electron Beam Accelerator Facility (CEBAF), presently under construction, consists of a pair of .4 GeV recirculating linacs and will produce a 4 GeV CW beam with average currents of up to 200  $\mu$ A. Because the accelerator is recirculating, multiple beams of different energies are present simultaneously in the linac beamlines. In these sections, it is required that the position of each different energy beam be measured separately. To achieve this, the electron beam itself must be modulated in time in such a way that each different energy beam in the linacs induces signals on the beam position monitors (BPMs) that can be separated using correlation techniques.

In this paper, two types of correlation receiving systems used at CEBAF for the linac BPMs are described in detail. These receivers are based on the pulsed and bi-phase pseudorandom modulated carrier methods for modulating the electron beam. In addition, the BPM receivers for the CEBAF arc regions, where the different energy beams are physically separated, are also described.

## OVERVIEW

The Continuous Electron Beam Accelerator Facility (CEBAF) is a five pass recirculating electron accelerator with an energy gain of 800 MeV per pass.<sup>1</sup> The accelerator itself consists of a pair of 400 MeV CW linacs connected together by two sets of five recirculating arcs stacked on top of one another. Each linac consists of 20 superconducting accelerating modules with energy gains of 20 MeV each. The beam characteristics relevant to the Beam Position Monitor (BPM) system are as follows:

- |                                    |  |
|------------------------------------|--|
| 1) Fundamental RF frequency        | $f_o = 1.497$ GHz                                |
| 2) Bunch length ( $1^\circ$ of RF) | $\tau_b = 1.85$ psec                             |
| 3) Average beam current            | $1 \mu\text{A} \leq I_{av} \leq 200 \mu\text{A}$ |
| 4) Recirculation time              | $\tau = 4.2$ $\mu$ sec                           |
| 5) CW with 1 bunch per RF cycle    |  |

As indicated in figure 1, the five different energy beams reside in separate vacuum chambers in the arcs. However, in the linacs, all five energies (passes) reside in the same beampipe. In order to tune up the machine and perform

---

\* This work was supported by the U.S. Department of Energy under contract DE-AC05-84ER40150.

periodic orbit corrections, it is necessary to track beam position through the entire five pass orbit.<sup>2</sup> In the CEBAF arcs, this can be accomplished with standard position monitoring techniques. In the linacs, the problem is complicated by the fact that five different energy beams following five different paths are present simultaneously in the same beampipe. In order to distinguish between passes in the linacs, it is necessary to mark or modulate the beam in a controlled manner so that the beam current for each pass in the linacs possesses unique characteristics.

In order to disturb experimental processes in the end stations as little as possible, it is necessary to modulate the beam current only when an actual orbit correction is being performed. Therefore, the CEBAF BPM system actually consists of two subsystems, one for the arc regions and one for the linacs. The arc system consists of pickups and receivers which operate at the fundamental RF frequency of 1.497 GHz. These BPMs monitor beam position in each of the five arcs continuously. Because beam optics in the arc regions are more critical than linac optics, a drift requiring orbit correction is most pronounced in the arcs. In the event that a drift severe enough to require a global orbit correction is detected in the arcs, the beam modulation and linac BPM system can be activated. With beam position information for the entire machine available for each pass, an orbit correction can then be performed.

It is presently estimated that 400-600 BPMs are required for the CEBAF arcs. In addition, there are 25 BPMs in each linac. Because of the large number of monitors involved, low cost designs for pickups and receivers are of primary concern. It is also a requirement to measure beam position to an accuracy of .1 mm with intensities as low as 1  $\mu\text{A}$ . Therefore, it is important that the pickups are highly sensitive and that the receivers exhibit low signal-to-noise characteristics. Features common to both the linac and arc systems for achieving these goals include simple high impedance - low cost stripline pickups and synchronous heterodyne receivers.

Quite fortunately, the larger of the two BPM systems, that of the arcs, is also the simpler. In this system, the pickups consist of open-ended thin-wire striplines<sup>3</sup> tuned to the fundamental RF frequency of 1.497 GHz. At this frequency, the magnitude of the beam current is  $2I_{av}$  and can range from 2  $\mu\text{A}$  to 400  $\mu\text{A}$  peak. The arc monitor receivers synchronously demodulate the 1.497 GHz signals from the pickups, in two stages, to DC. The standard difference-over-sum technique is then used to determine beam position. Because bandwidth requirements in the arcs are essentially zero, extremely high accuracy with very low beam currents can be obtained.

As previously mentioned, the position of each of the five different energy beams present in the linacs must be determined separately. Therefore, at the injector, the beam must be marked or encoded in such a way that each pass in the linacs can be distinguished. As a first step, a 100 MHz, 1  $\mu\text{A}$  amplitude modulation is impressed on the beam at the grid of the injector electron gun.

periodic orbit corrections, it is necessary to track beam position through the entire five pass orbit.<sup>2</sup> In the CEBAF arcs, this can be accomplished with standard position monitoring techniques. In the linacs, the problem is complicated by the fact that five different energy beams following five different paths are present simultaneously in the same beampipe. In order to distinguish between passes in the linacs, it is necessary to mark or modulate the beam in a controlled manner so that the beam current for each pass in the linacs possesses unique characteristics.

In order to disturb experimental processes in the end stations as little as possible, it is necessary to modulate the beam current only when an actual orbit correction is being performed. Therefore, the CEBAF BPM system actually consists of two subsystems, one for the arc regions and one for the linacs. The arc system consists of pickups and receivers which operate at the fundamental RF frequency of 1.497 GHz. These BPMs monitor beam position in each of the five arcs continuously. Because beam optics in the arc regions are more critical than linac optics, a drift requiring orbit correction is most pronounced in the arcs. In the event that a drift severe enough to require a global orbit correction is detected in the arcs, the beam modulation and linac BPM system can be activated. With beam position information for the entire machine available for each pass, an orbit correction can then be performed.

It is presently estimated that 400-600 BPMs are required for the CEBAF arcs. In addition, there are 25 BPMs in each linac. Because of the large number of monitors involved, low cost designs for pickups and receivers are of primary concern. It is also a requirement to measure beam position to an accuracy of .1 mm with intensities as low as 1  $\mu$ A. Therefore, it is important that the pickups are highly sensitive and that the receivers exhibit low signal-to-noise characteristics. Features common to both the linac and arc systems for achieving these goals include simple high impedance - low cost stripline pickups and synchronous heterodyne receivers.

Quite fortunately, the larger of the two BPM systems, that of the arcs, is also the simpler. In this system, the pickups consist of open-ended thin-wire striplines<sup>3</sup> tuned to the fundamental RF frequency of 1.497 GHz. At this frequency, the magnitude of the beam current is  $2I_{av}$  and can range from 2  $\mu$ A to 400  $\mu$ A peak. The arc monitor receivers synchronously demodulate the 1.497 GHz signals from the pickups, in two stages, to DC. The standard difference-over-sum technique is then used to determine beam position. Because bandwidth requirements in the arcs are essentially zero, extremely high accuracy with very low beam currents can be obtained.

As previously mentioned, the position of each of the five different energy beams present in the linacs must be determined separately. Therefore, at the injector, the beam must be marked or encoded in such a way that each pass in the linacs can be distinguished. As a first step, a 100 MHz, 1  $\mu$ A amplitude modulation is impressed on the beam at the grid of the injector electron gun.

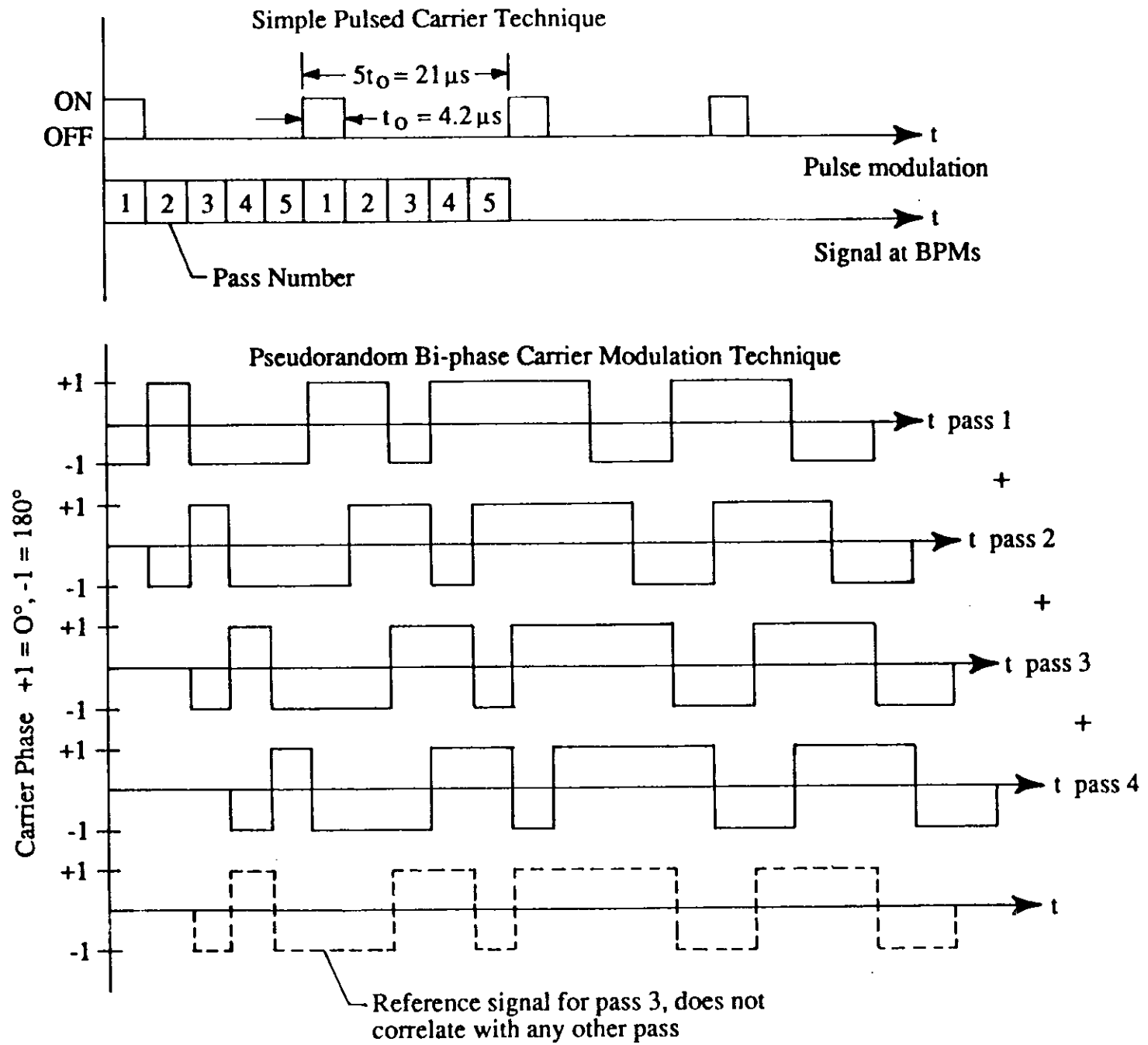


Figure 2. Simple pulse and pseudorandom modulation for spreading linac passes.

pickups themselves are thoroughly described in the references mentioned above and will not be addressed here. Both the simple pulsed linac system (presently being used at CEBAF) and the pseudorandom sequence system (planned upgrade) will be discussed in detail with experimental results given.

### 100 MHz LINAC RECEIVERS (SIMPLE PULSED VERSION)

The first linac BPM system developed at CEBAF (presently used in the north linac) uses the simple pulsed 100 MHz carrier technique. A system diagram of the pulsed 100 MHz beam position monitor electronics is shown in figure 3. For optimum S/N, the system uses synchronous detection<sup>5</sup> to convert the 4.2 microsecond current modulation bursts detected by the four BPM pickups into pulses that are read with an analog-to-digital converter. The basic system components are: the matching network and tunnel line driver board, the synchronous detector board, and the integrate-and-dump and microprocessor board. Each of these components is described below.

A schematic for the tunnel line driver board is shown in figure 4. The matching networks resonate the BPM pickups and match them to 50 ohms, at 100 MHz. The matching networks consist simply of a capacitor for resonating the pickup and an impedance transformer. The networks, located right on the vacuum feedthroughs of the beam position monitor, are connected to the tunnel line driver board by several feet of 50 ohm cable. The matching networks are necessary for several reasons. The first and most obvious is that the input impedance of the amplifiers used on the tunnel line driver board is 50 ohms and a perfect match will couple the maximum amount of power from the loops into the amplifiers. This increases the signal-to-noise ratio of the system. In addition, a matched system allows the tunnel line driver board, which contains radiation sensitive active components, to be placed several feet away from the beam pipe. Lastly, a front end shunt capacitance in the networks resonates the BPM pickups for higher sensitivity.

The tunnel line driver board is used to amplify (20 dB) the 100 MHz signal detected by the loop prior to transport from the accelerator tunnel to the above-ground service buildings. A line driver is necessary because the distance between the monitor and the detector electronics in the service buildings can be several hundred feet. The use of a front end line driver and gain stage allows the signal to be transported many hundreds of feet without a serious degradation in the system noise figure. The L-C networks on the outputs of each channel of the board match the 50 ohm amplifiers to the 75 ohm RG-6/U cable that is used to transport the signal from the tunnel to the service buildings. It should be pointed out that RG-6/U cable is used for these long runs because it is considerably lower in cost than most 50  $\Omega$  cable.

A closer examination of the schematic shown in figure 4 reveals that there are two diode switches that are used to switch the autocalibration signals into

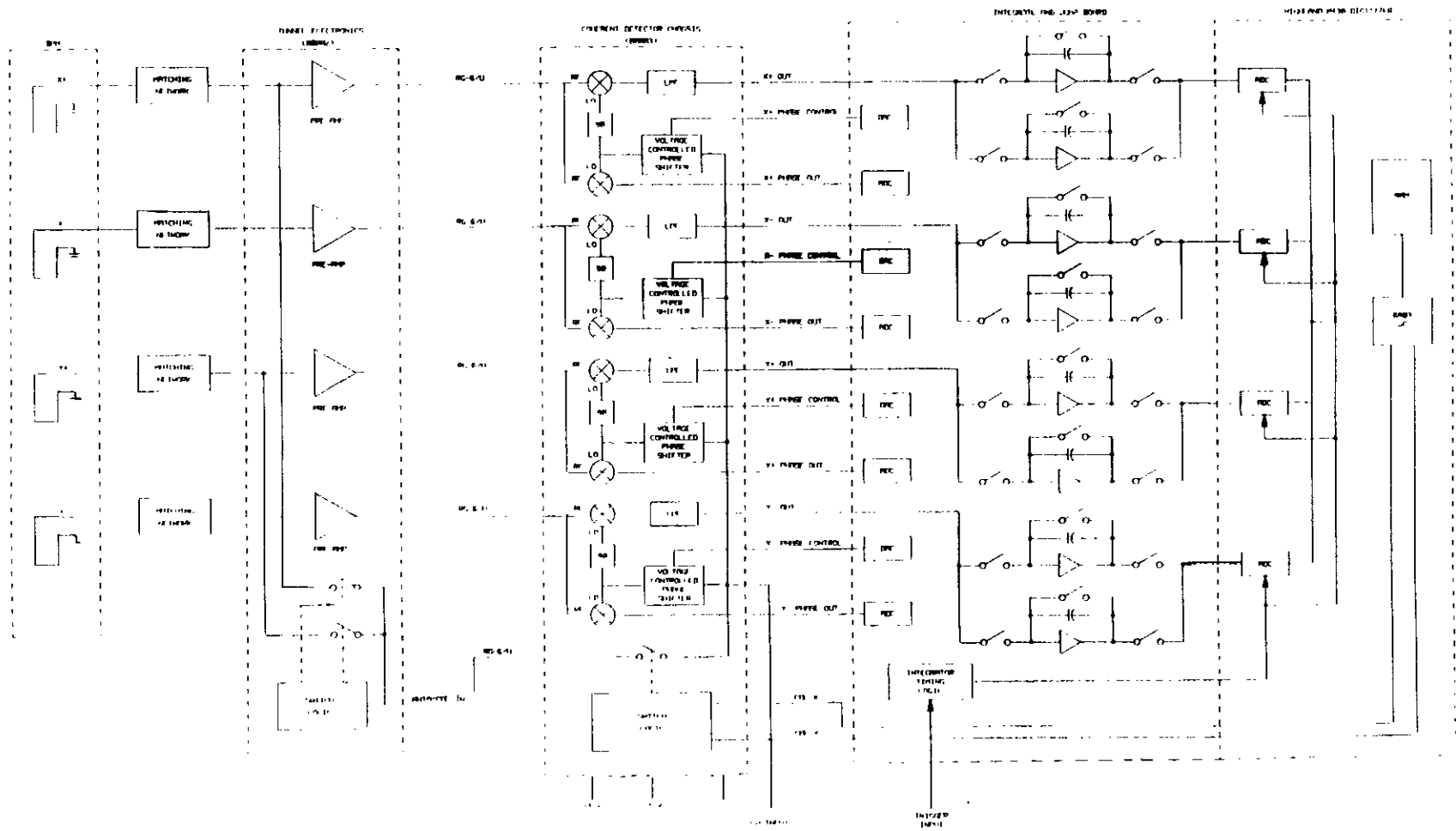


Figure 3. 100 MHz pulsed receiver system diagram.

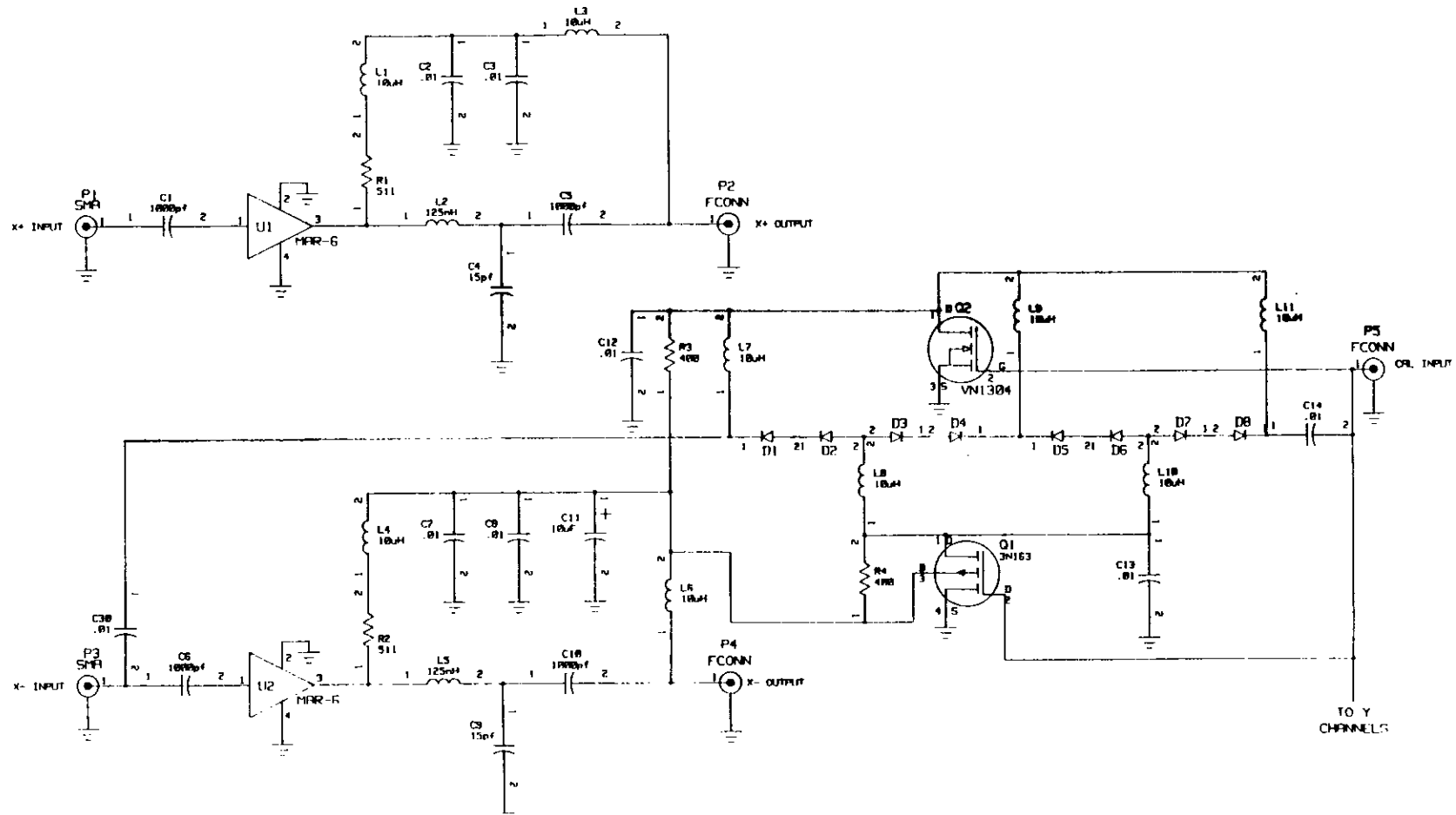


Figure 4. Tunnel line driver board.

the BPM. The autocalibration function of the system is discussed later in this paper. Another unique feature of the tunnel line driver board is that the power for the active components is supplied to the board from the coherent detector board through the output coax cables connecting the two. This dual usage of the cables reduces the number of cables that are required to be pulled through the already crowded penetrations that connect the service buildings to the tunnel.

A schematic of the coherent (synchronous) detector board is shown in figure 5. There are five basic parts to the board: RF amplifiers, voltage-controlled phase shifters for the local oscillator signals, quadrature phase detectors, down conversion mixers, and baseband amplifiers. The board is located in the above-ground service building and is used to convert the 100 MHz signal to baseband so it can be read with an analog-to-digital converter. Signals from the tunnel board are amplified by two stages of Mini-Circuits MAR-6 amplifiers. The gain of each stage is approximately 20 dB. The amplified signals are then down converted to baseband using an SBL-1 Mini-Circuits mixer. The local oscillator port of the mixer is driven by a Plessey SL952 limiting amplifier. Baseband signals from the IF port of the mixer are then amplified and passed to the Integrate-and-Dump Board. The gain of the baseband amplifiers is adjusted such that the total gain for the board from input to output is 75 dB.

The local oscillator signal used for the synchronous detector is derived from the same master oscillator that impresses the 100 MHz modulation on the beam at the injector gun. The signal is routed to each of the coherent detector boards via RG-6/U cable and coaxial cable couplers similar to those used in cable television systems. The local oscillator signal for each of the four channels on the board is phase shifted using the voltage-controlled varactor phase shift networks in figure 5. Four separate phase shifters were used in order to account for and eliminate phase differences between each of the four signals coming from each BPM. These channel-to-channel phase errors are due to matching network mismatches, differences in cable lengths, and differences in amplifiers. The varactor networks are capable of providing a full 360 degrees of phase shift at 100 MHz for a 1 to 10 volt control signal input. Each channel of the coherent detector board also uses a Motorola MC1496 multiplier as a phase detector. The phase detector output is passed to the Integrate-and-Dump Board and is used by the CEBAF control system to phase lock each of the channels. The phase lock algorithm is discussed later in this paper.

The schematic representation for the Integrate-and-Dump Board is shown in figure 3. The board resides in a CAMAC crate slot next to the microprocessor board and has several functions: integration of the baseband signal from the coherent detector board over the 4.2 microsecond modulation burst, analog-to-digital conversion of the phase detector signals for each channel, digital to analog conversion of the phase adjust signals for each channel, CAMAC interface to the control system computer for these signals, and timing circuitry for the integrators and analog-to-digital converters on the microprocessor board.

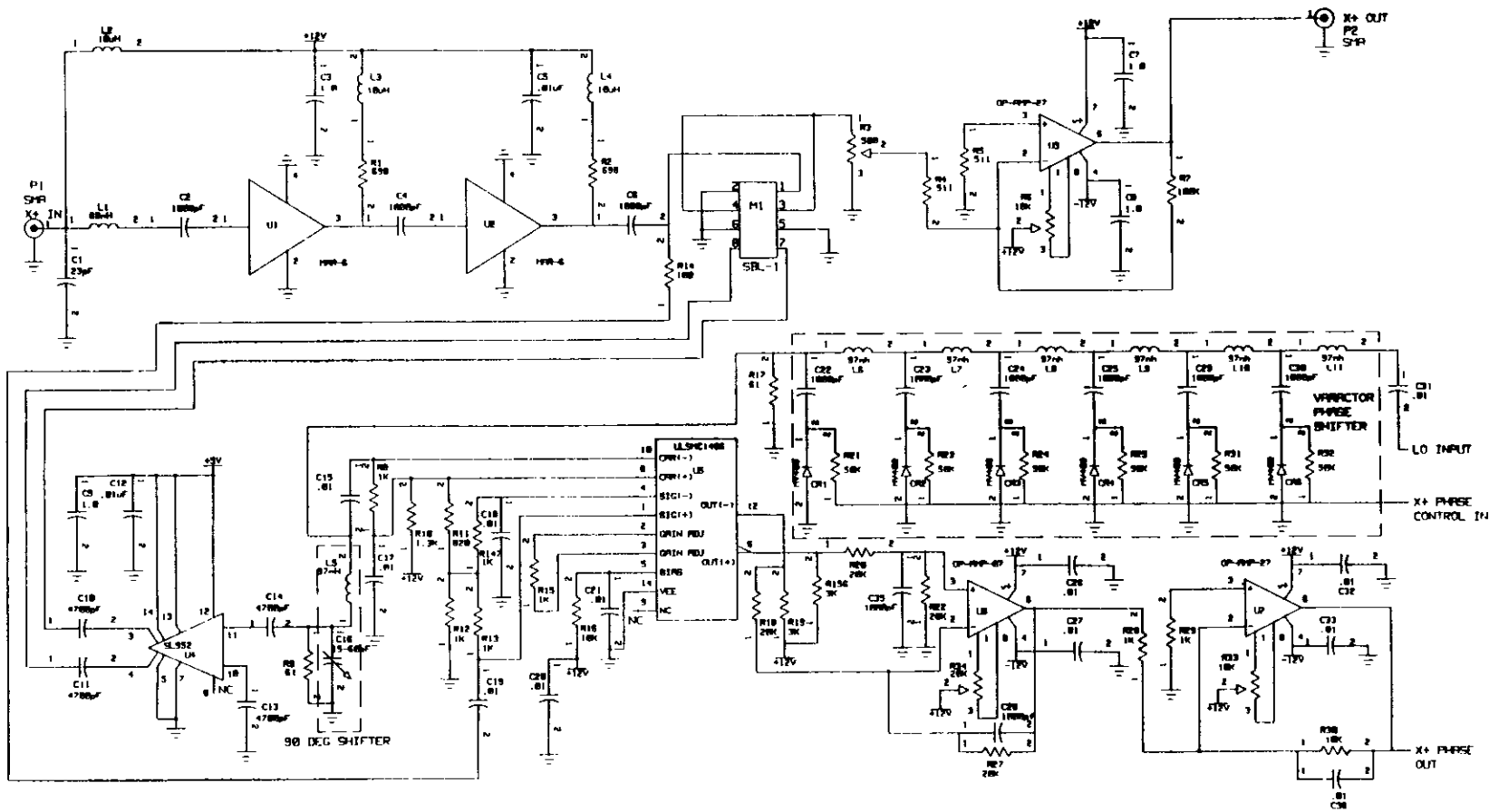


Figure 5. Coherent detector board.

Each channel of the coherent detector board feeds dual integrators on the Integrate-and-Dump Board. The integrate-and-dump technique was used because it provides an optimal filter for a pulse such as that produced during a modulation burst.<sup>6,7</sup> The dual integrators allow the board to acquire each of the five passes every time the current modulation is injected into the accelerator. A timing diagram for the integration of each pass is shown in figure 6. As can be seen, integrator number 1 integrates the first burst. At the end of 4.2 microseconds the integration is held and the analog-to-digital converter on the microprocessor board is triggered. Meanwhile integrator number 2 is integrating the second burst. Once the ADC has finished with burst 1, the integrator is dumped and readied to integrate burst 3. This sequence continues until all five bursts have been integrated and digitized.

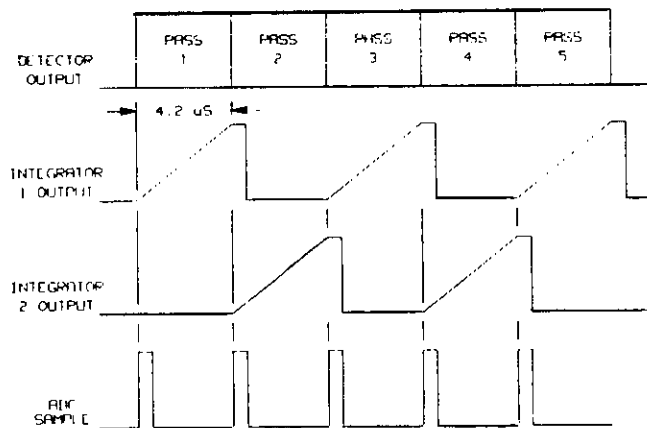


Figure 6. 100 MHz BPM Integrate-and-Dump Board timing diagram.

The microprocessor board used for the 100 MHz BPMs is a Highland Technologies model M430 eight channel digitizer module. It is a single width CAMAC module that uses a Motorola 6803 microprocessor and eight fast analog-to-digital converters to digitize the signals fed to it from the Integrate-and-Dump Board. The module can store up to 256 data points for each of the five passes. Once the data are stored in buffer memory, the microprocessor can perform various filtering and averaging operations and calculate the position of each of the five beam passes. The microprocessor also controls the autocalibration of each monitor channel and uses the offset and relative gain data acquired from the calibration for the beam position calculation. The actual signal processing and calibration algorithms are described below.

The 100 MHz BPM receiver has a built-in autocalibration function. The autocalibration function is used to check the offset and relative gain of each of the four channels and is controlled by the microprocessor module. The autocalibration sequence is as follows (refer to figure 3):

1. The CEBAF control system commands the microprocessor to perform a system calibration. The command is issued over the CAMAC bus.

2. The microprocessor module then reads the offset voltage of each of the four BPM channels. This reading is taken in the absence of beam modulation and with no signal applied to the loops. The offset voltage for each channel is stored in memory.
3. The microprocessor then sets a bit indicating that a portion of the local oscillator signal should be split off at each coherent detector and sent to the tunnel board. If the  $X$  channels are being calibrated, the diode switch connected to the  $Y^-$  channel of the tunnel board is closed and the signal is sent to the  $Y^-$  loop. The switch is controlled by a DC bias applied to the autocalibration signal line. Each of the  $X$  loops of the BPM picks up this signal. The control computer then performs the phase lock algorithm described below. After the system has been locked, the microprocessor reads the voltage of the  $X$  channels with the ADCs and calculates the relative gain of each channel. Again, this process is performed in the absence of beam modulation.
4. The sequence is repeated for the  $Y$  channels. The relative gains for each channel are then stored in memory.

The type of calibration described above checks the gain and offset of all components of each channel and is performed each time a position measurement is to be made or when the system accuracy is in question. Inherent in the calibration technique used is the assumption that all gain and offset drifts are slow and negligible on the time scale of the measurement. This is a reasonable assumption because most gain and offset drifts are induced by changes in ambient temperature which are indeed small on the time scale of a few seconds.

The Highland Model M430 Digitizer module is capable of performing various signal processing algorithms and position calculations. At this time the only signal filtering that is used is an averaging algorithm. The control computer instructs the module how many measurements of each of the signals are to be averaged. The maximum number of averages is presently set at 256. Each of the signal averaging calculations is performed to 16 bit accuracy. In the future, the microprocessor will perform the correlation function that will be used in conjunction with the pseudorandom modulation technique described elsewhere in this paper.

The module also performs the actual position calculation for each of the five beam passes. The position calculation is performed to 16 bit accuracy and is given by equations 1 and 2.

$$X_{pos} = K_{BPM} \frac{K_{x+}(X^+ - X_{off}^+) - K_{x-}(X^- - X_{off}^-)}{K_{x+}(X^+ - X_{off}^+) + K_{x-}(X^- - X_{off}^-)} \quad (1)$$

$$Y_{pos} = K_{BPM} \frac{K_{y+}(Y^+ - Y_{off}^+) - K_{y-}(Y^- - Y_{off}^-)}{K_{y+}(Y^+ - Y_{off}^+) + K_{y-}(Y^- - Y_{off}^-)} \quad (2)$$

where  $K_{x+}, K_{x-}, K_{y+}, K_{y-}$  are the relative gain coefficients of each channel, determined during auto-cal.

$X_{off}^+, X_{off}^-, Y_{off}^+, Y_{off}^-$  are the offsets of each channel, determined during auto-cal.

$X^+, X^-, Y^+, Y^-$ , are the processed values for each channel and pass.

$K_{BPM}$  is the constant relating difference-over-sum voltage ratio to beam position for the BPM.

The CEBAF 100 MHz BPM electronics are phase locked to the beam modulation and the autocalibration signal by the control computer. A flowchart for the algorithm is shown in figure 7. Phase locking of the system is performed at system startup, during autocalibration and whenever it is determined that the system phase has drifted. The basic procedure is as follows:

1. The modulation or autocalibration signal is turned on, and the phase detector output for each channel is read by the control computer through CAMAC.
2. The actual phase difference between the local oscillator and the signal is calculated.
3. The phase of the local oscillator is adjusted as per the algorithm using a digital-to-analog converter and the varactor phase shifter for each channel.
4. This process is repeated until the phase difference is less than 2 degrees. The DAC voltage is then held constant until a new phase adjustment is necessary.

The phase locking technique described above, like the autocalibration algorithm, relies upon the assumption that drifts in phase are slow and negligible during the time period of a measurement or series of measurements.

The 100 MHz system described above was tested using the CEBAF injector during July of 1990. The tests included tests of the actual system components and the phase-lock and autocalibration algorithms. In addition, this system is installed and will be used in the Front End Test and commissioning of the north linac.

The performance of the BPM was examined to the extent possible by comparing position readings from the BPM with those determined with a standard phosphorescent view screen located next to the BPM in the beamline. The view screen, normally used for rough visual feedback when steering and focussing the beam, is not absolutely calibrated with respect to the center of the beamline. In addition, persistence and blooming, which enlarge the apparent spot size of the beam, further degrade the accuracy of beam position measurements with the view screen. These effects, combined with position readings obtained from a TV monitor, make the view screen method of measuring beam position approximate at best. However, it was still of qualitative importance to compare BPM readings with beam position as measured with the view screens. The re-

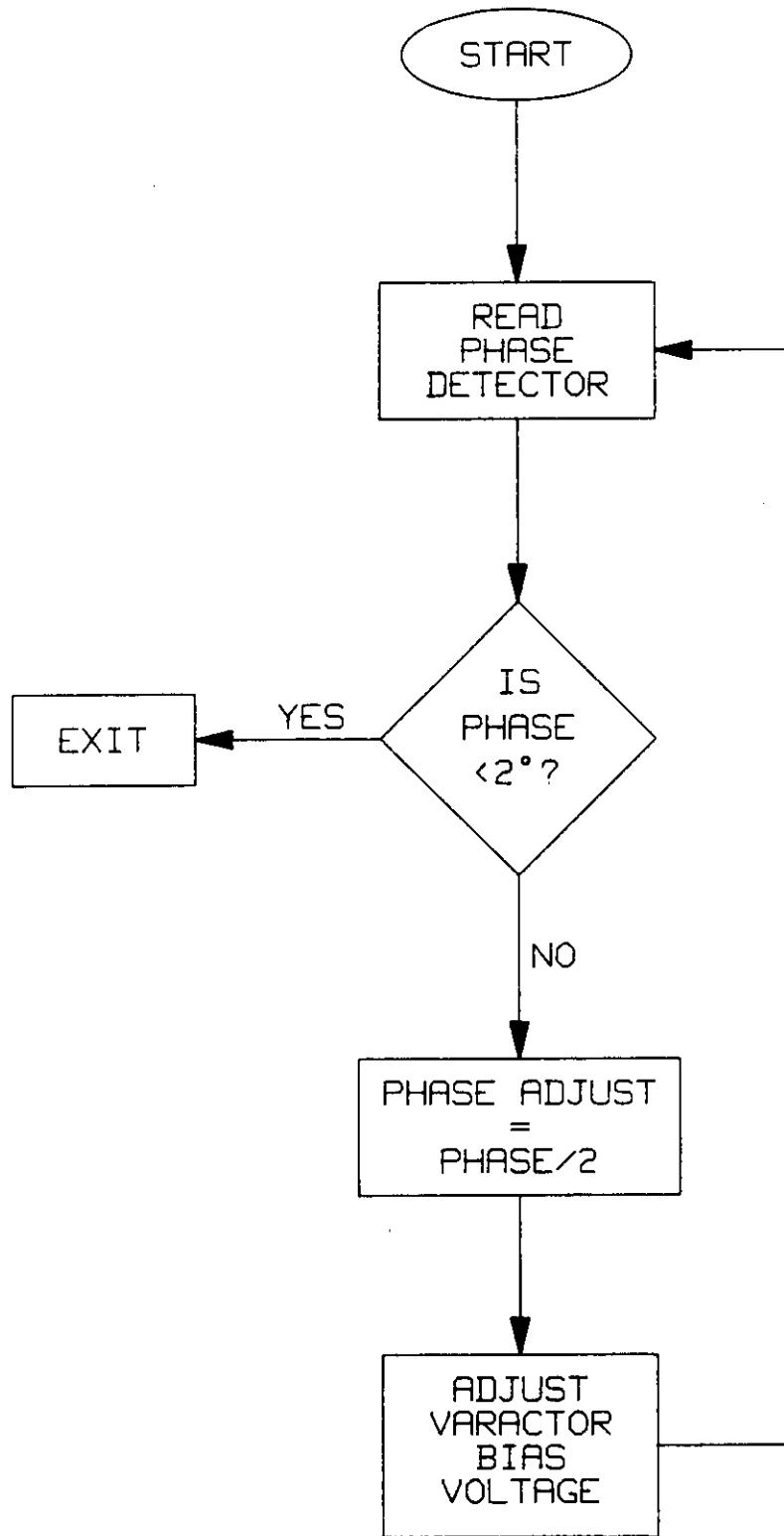


Figure 7. Phase lock algorithm.

sults of such a comparison appear in figure 10. Here, the beam was positioned with x and y steering coils about a square grid in 4 mm increments as determined by view screen readings (dots). The associated BPM readings for each position are indicated by crosses in figure 8. As shown, qualitative agreement exists between the two devices. Note: Due to beam steering difficulties data could not be obtained for positions  $(-4, 4)$ ,  $(4, 4)$ , and  $(4, -4)$ .

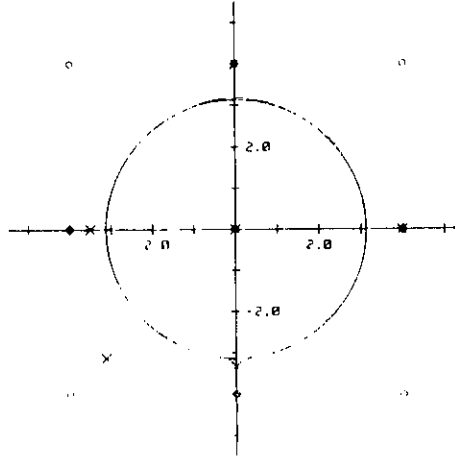


Figure 8. 100 MHz BPM injector test results  
 X = BPM measured position. O = Viewer measured position.  
 Large circle is beam spot size on viewer.

A system diagram of the 1497 MHz arc monitor electronics is shown in figure 9. The system uses a down converter and phase locked loop to detect the amplitude of each of the four monitor signals. The basic system components are the tunnel board which down converts the 1497 MHz signal to 1 MHz and the detector board which contains the phase locked loops and analog-to-digital converters. The control computer uses the ADC data to calculate the beam position.

A schematic of the tunnel board is shown in figure 10. The purpose of the board is to down convert the 1497 MHz beam signal to 1 MHz prior to transport to the detector board. The two Mini-circuits MAR-6 amplifiers on the front end of each channel amplify the 1497 MHz signal approximately 17 dB prior to down conversion. The 1496 MHz local oscillator is a Wilmanco model 4S-U-1496/PC. Following down conversion, the 1 MHz signal is amplified and sent to the detector board via RG-6/U cable.

The tunnel board is used to synthesize and inject the calibration signal during autocalibration. The 20 dB microstrip couplers and RF switches are used to inject the signal on the appropriate wire. The autocalibration algorithm is described later in this paper.

A block diagram representation of the detector board is shown in figure 9. The electronics are housed in a single width CAMAC module located in the above-ground service buildings. The main purpose of the board is to detect



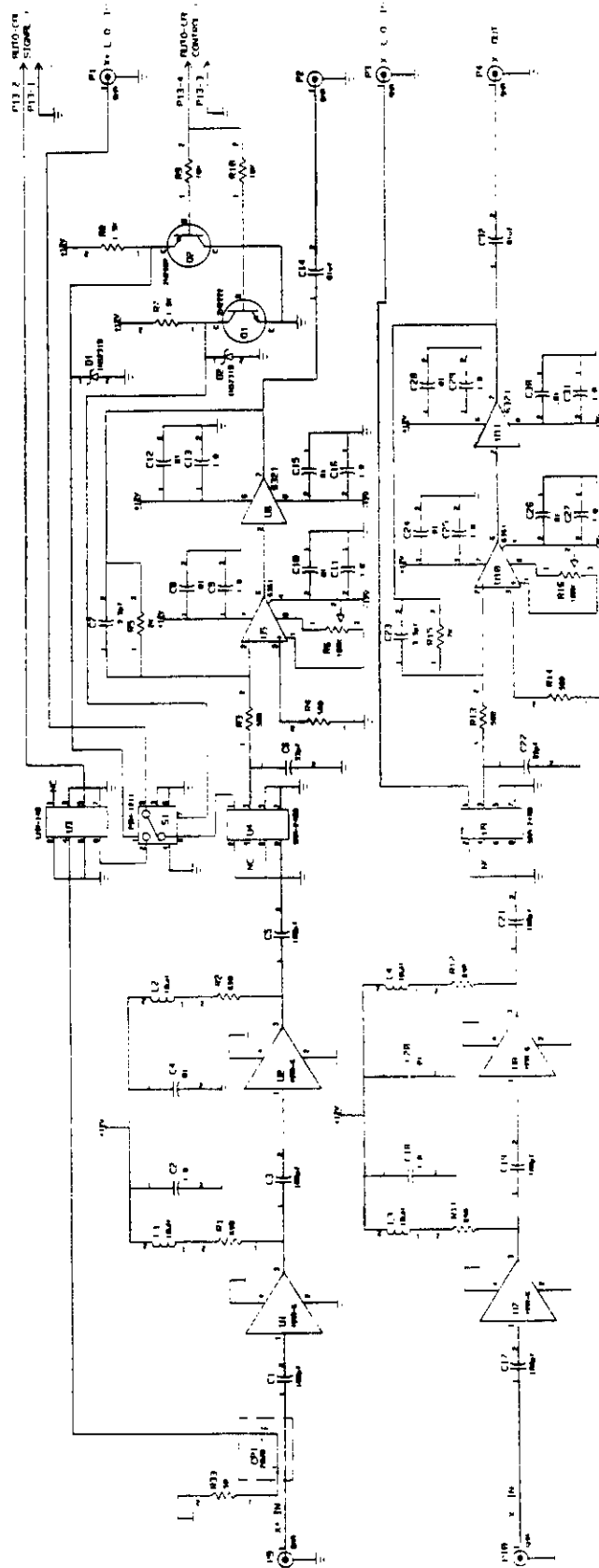


Figure 10. 1497 MHz tunnel electronics.

the amplitude of each of the four BPM signals and provide the CAMAC interface for the system. The front end amplifier for each channel is a Motorola MC1490 programmable-gain amplifier. The amplifier gains are controlled with a quad DAC. The 1497 MHz BPM detector board requires a programmable or adjustable gain because, unlike the 100 MHz BPM, the 1497 MHz BPM must operate over a variety of beam currents (from 1 to 200 microamps). The control computer adjusts the gain of the amplifier according to the accelerator beam current.

The heart of the detector board is the Signetics NE564 phase locked loop chip. The NE564 locks to the incoming 1 MHz signal at the output of each of the programmable gain amplifiers. The lock time for the NE564 is less than 50 microseconds. The VCO output signal from the NE564 and the 1 MHz signal from each programmable amplifier are then multiplied using a Motorola MC1496 multiplier. The output of the multipliers are low-pass filtered and sampled using ADCs.

The control computer reads the amplitude of each of the BPM signals via the ADCs and CAMAC. The module can also be programmed from CAMAC for single or continuous ADC scanning. In the single-scan mode the trigger for the ADC is provided from an external source via a front panel connector. Autocalibration functions, which are described below, are also controlled by the control computer via CAMAC.

The following discussion refers to circuits shown in figures 9 and 10. The 1497 MHz BPM electronics are calibrated in much the same way as the 100 MHz BPM. A major difference is that the beam must be turned off for 1497 MHz autocalibration so as not to interfere with the injected signals. A signal is injected onto a BPM pickup and is read back through the channels in the opposite BPM plane. The computer can then calculate the relative gain and offset of each channel and use these coefficients in the position calculations of equations 1 and 2. There are only a few differences in the actual implementation.

The 1497 MHz BPM system does not have a local oscillator signal that is distributed around the accelerator; therefore the 1497 MHz calibration signal must be synthesized. A 1 MHz oscillator is located on the detector board. This signal is sent to the tunnel board via RG-6/U cable. On the tunnel board this signal is mixed with the 1496 MHz local oscillator signal. The resulting sum frequency (1497 MHz) signal is then coupled into the pickup via a 20 dB microstrip coupler. The RF switches on the tunnel board which direct the local oscillator signal to the appropriate mixers are controlled by signals from the detector board. It should also be noted that the amplitude of the 1 MHz oscillator signal on the detector board is adjustable from CAMAC. This is done in an attempt to simulate the various beam currents over which the BPM electronics are required to operate.

The 1497 MHz detector and tunnel amplifier boards were tested during July of 1990 on the CEBAF injector. The on-line autocalibration function was not ready at the time, although the system was calibrated by injecting a 1497 MHz

signal from a signal generator into a BPM pickup and recording the offset and relative gain of each channel. The tests were conducted in the same manner as described in the 100 MHz test results section of this paper, and for the same reasons the results can only be used to qualitatively verify operation. Figure 11 is a plot of BPM position readings versus a 4 mm square grid measured on the view screen. As shown, qualitative agreement does exist between the BPM readings and the view screen positions.

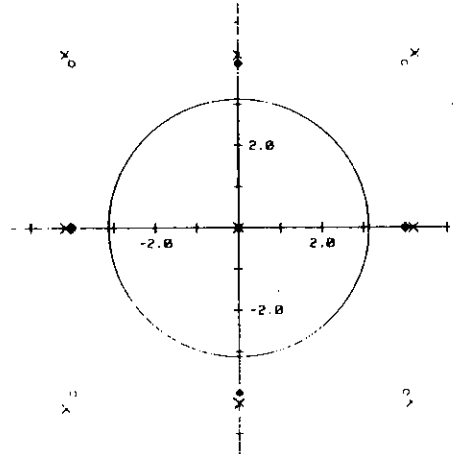


Figure 11. 1497 MHz injector test results  
 X = BPM measured position. O = Viewer measured position.  
 Large circle is beam spot size on viewer.

### 100 MHz BI-PHASE PSEUDORANDOM MODULATION TECHNIQUE FOR LINACS

As described in previous sections, one way to measure each beam individually is to modulate the beam for a period of less than or equal to the revolution time,  $4.2 \mu\text{sec}$ . The signal will appear sequentially as the modulated pulse passes a BPM on each of the passes through the linac. The first signal corresponds to the lowest energy pass, the second to the next higher energy pass, and so on. Although this method provides a straightforward measurement of the position of the beam in each pass, it has the disadvantage that each measurement for each pass can only be made once every five revolution periods ( $21 \mu\text{sec}$ ).

Recently another solution to the problem of individual beam position measurement has been devised.<sup>8</sup> In this method, the 100 MHz carrier is turned on continuously, but the carrier phase is switched from  $0^\circ$  to  $180^\circ$  every revolution period,  $\tau$ , in such a way that each pass can be distinguished with no interference from other passes.

The separate identification of each beam can be illustrated for the simple case of two passes. Let us assume a modulation amplitude

$$f(t) = A \sin(\omega t) x(t/\tau), \quad (3)$$

where  $\omega$  is the 100 MHz modulation frequency,  $\tau$  is the beam circulation period in the machine (4.2  $\mu$ s for CEBAF), and  $x(t/\tau)$  is a function with values  $\pm 1$ , changing at integer values of its argument. Consider the sequence

$$x = 1, 1, -1, -1, 1, 1 - 1, -1, \dots \quad (4)$$

where  $\pm 1$  corresponds to a  $0^\circ$  and  $180^\circ$  phase shift of the carrier. If the signal is mixed with itself, the resulting product is

$$f(t)f(t) = A^2 \sin^2(\omega t), \quad (5)$$

which represents the detected signal for the first pass. The time average is nonvanishing and is equal to  $A^2/2$ . If  $f(t)$  is delayed by  $\tau$  (second pass) and then mixed with the undelayed signal, the product is:

$$f(t)f(t - \tau) = A^2 \sin^2(\omega t) x(t/\tau) x(t/\tau - 1). \quad (6)$$

The time average is then

$$\begin{aligned} \frac{1}{T} \int_0^T f(t)f(t - \tau) dt &= \frac{A^2}{T} \int_0^T \sin^2(\omega t) dt (1 - 1 + 1 - 1 \dots) \\ &\approx 0. \end{aligned} \quad (7)$$

Thus, the correlation function in this case picks out the signal from the first pass and suppresses that from the second. To suppress the first and observe the second, the signal is mixed with the delayed sequence  $f(t - \tau)$ .

The sequence  $x(t/\tau)$  that has been given for illustrative purposes is not sufficient for three or more passes, but it is easy to extend the argument. It is necessary only to generate a sequence with values  $\pm 1$  such that the autocorrelation function with delay will vanish. Such sequences are already well known in coding theories for communications systems where they are referred to as pseudorandom sequences.

The correlation function  $R(x, y; n)$  is defined as

$$R(x, y; n) = \frac{1}{T} \int_0^T x(t/\tau) y(t/\tau + n) dt, \quad (8)$$

where  $x(t/\tau)$ ,  $y(t/\tau)$  are pulse sequences with values  $\pm 1$ ,  $T$  is the total time of the sequence, and  $n\tau$  is the time delay. We are particularly interested in the autocorrelation,  $x(t/\tau) = y(t/\tau)$ , which should satisfy the following orthogonality condition in order for the sequence to act as a filter:

$$\begin{aligned} R(x, x; n) &= \frac{1}{T} \int_0^T x(t/\tau) x(t/\tau + n) dt = 1 \text{ if } n = 0, \\ &= 0 \text{ if } n \neq 0. \end{aligned} \quad (9)$$

where  $\omega$  is the 100 MHz modulation frequency,  $\tau$  is the beam circulation period in the machine (4.2  $\mu$ s for CEBAF), and  $x(t/\tau)$  is a function with values  $\pm 1$ , changing at integer values of its argument. Consider the sequence

$$x = 1, 1, -1, -1, 1, 1 - 1, -1, \dots \quad (4)$$

where  $\pm 1$  corresponds to a  $0^\circ$  and  $180^\circ$  phase shift of the carrier. If the signal is mixed with itself, the resulting product is

$$f(t)f(t) = A^2 \sin^2(\omega t), \quad (5)$$

which represents the detected signal for the first pass. The time average is nonvanishing and is equal to  $A^2/2$ . If  $f(t)$  is delayed by  $\tau$  (second pass) and then mixed with the undelayed signal, the product is:

$$f(t)f(t - \tau) = A^2 \sin^2(\omega t) x(t/\tau) x(t/\tau - 1). \quad (6)$$

The time average is then

$$\begin{aligned} \frac{1}{T} \int_0^T f(t)f(t - \tau) dt &= \frac{A^2}{T} \int_0^T \sin^2(\omega t) dt (1 - 1 + 1 - 1 \dots) \\ &\approx 0. \end{aligned} \quad (7)$$

Thus, the correlation function in this case picks out the signal from the first pass and suppresses that from the second. To suppress the first and observe the second, the signal is mixed with the delayed sequence  $f(t - \tau)$ .

The sequence  $x(t/\tau)$  that has been given for illustrative purposes is not sufficient for three or more passes, but it is easy to extend the argument. It is necessary only to generate a sequence with values  $\pm 1$  such that the autocorrelation function with delay will vanish. Such sequences are already well known in coding theories for communications systems where they are referred to as pseudorandom sequences.

The correlation function  $R(x, y; n)$  is defined as

$$R(x, y; n) = \frac{1}{T} \int_0^T x(t/\tau) y(t/\tau + n) dt, \quad (8)$$

where  $x(t/\tau)$ ,  $y(t/\tau)$  are pulse sequences with values  $\pm 1$ ,  $T$  is the total time of the sequence, and  $n\tau$  is the time delay. We are particularly interested in the autocorrelation,  $x(t/\tau) = y(t/\tau)$ , which should satisfy the following orthogonality condition in order for the sequence to act as a filter:

$$\begin{aligned} R(x, x; n) &= \frac{1}{T} \int_0^T x(t/\tau) x(t/\tau + n) dt = 1 \text{ if } n = 0, \\ &= 0 \text{ if } n \neq 0. \end{aligned} \quad (9)$$

Perfect sequences,<sup>9</sup> which satisfy equation 9 exactly, are hard to find and implement. Shift register sequences, however, which will satisfy equation 9 to within an arbitrarily small residual error determined by the length of the sequence, can be easily implemented by shift registers with appropriate feedback connections. Programmable array logic (PAL) devices can produce shift register sequences in a single device that needs only a clock pulse. A length-63 PRS generator is indicated in figure 12.

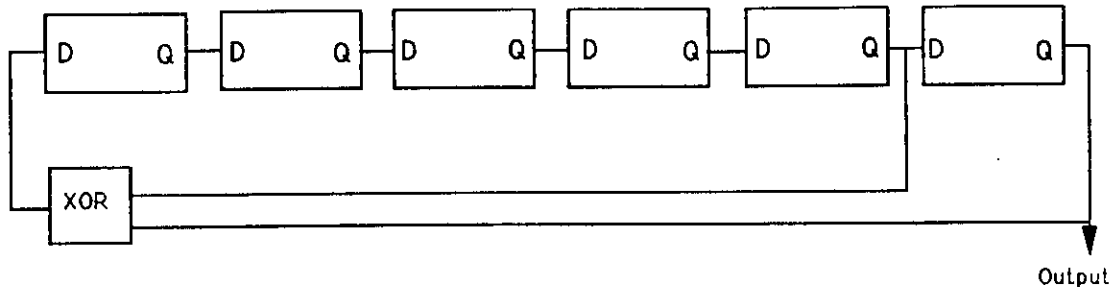


Figure 12. Shift register pseudorandom sequence generator (length 63).

The so-called maximal-length shift register sequence has nearly perfect autocorrelation characteristics. It is referred to as pseudorandom because it has several randomness characteristics<sup>10</sup>:

1. the numbers of +1 and -1 pulses are approximately equal, with a maximum difference of 1,
2. the number of runs of length  $l$  is proportional to  $2^{-l}$ ,
3. the autocorrelation function has only 2 values.

The first of these characteristics is convenient because it means that an electronic implementation will not have to compensate for large shifts in the voltage or current levels introduced by the PRS modulation. The second implies that the levels will not shift appreciably within the time span of the sequence; for example, the longest possible run for a PRS of length 1023 is 10 consecutive +1s or -1s, and this longest run will occur only once. The third is the required autocorrelation condition. The autocorrelation values for maximal-length sequences are

$$\begin{aligned}
 R &= \frac{1}{N} \sum_{r=0}^{N-1} x(r)x(r+n) = 1, \quad n = 0, \\
 &= -\frac{1}{N}, \quad n \neq 0.
 \end{aligned}
 \tag{10}$$

For sequences of reasonable length, the deviation from perfect autocorrelation is insignificant.

For a PRS that is generated by a shift register of  $n$  stages, the maximum length is  $2^n - 1$ . Note that the orthogonality condition is satisfied only for a complete sequence; a sum of less than a complete sequence will have spurious peaks. It is not usually difficult to use a complete sequence. The characteristics of a three-stage shift register that generates a length-7 pseudorandom sequence are illustrated in figure 13.

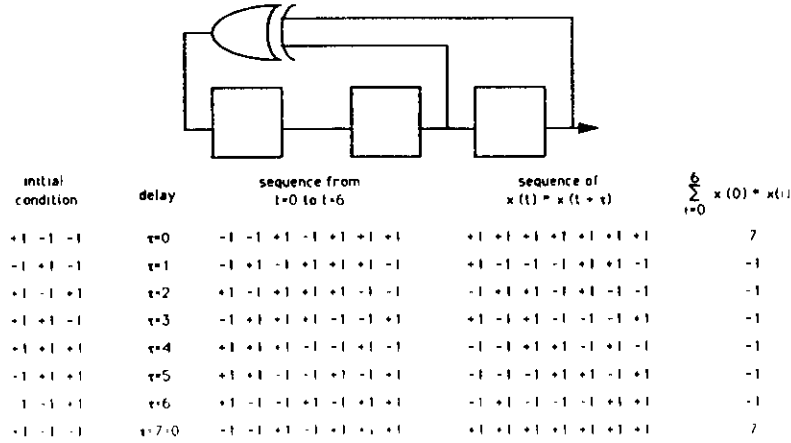


Figure 13. Orthogonality of shifted length-7 pseudorandom sequence.

Shift registers also provide another benefit in that they are easily expanded. Addition of another register stage will double the length of the maximal sequence, so with small expenditure one can select a sequence length that will give the processing time required to process the signal and average out the interference.

The block diagram for the pseudorandom modulation and detection is shown in figure 14. The beam is modulated with the frequency  $\omega$  and in addition by a pseudorandom sequence  $Ax(t)$ ,

$$I = I_0 + Ax(t/\tau) \sin(\omega t), \quad (11)$$

where  $x(t/\tau)$  is either +1 or -1. For five beam passes through the detector, the output signal at a BPM pickup is:

$$S_d = \sum_{r=0}^4 (k_r Ax(t/\tau - r) \sin(\omega t - r\tau)) + \text{noise}, \quad (12)$$

where  $k_r$  is a constant for each pass which depends upon its position. Because noise is generally quite system-specific and cannot be easily handled analytically,<sup>11</sup> we will henceforth neglect its effect; as usual, however, noise decreases with sequence length and will determine the processing time needed

for a given signal/noise ratio. When the detector signal is mixed with the input delayed by  $j$  circulation periods, the output is

$$S = \sum_{r=0}^4 k_r A^2 x(t/\tau - r) x(t/\tau - j) \sin^2(\omega t). \quad (13)$$

Integration over  $m$  complete sequences will remove the high-frequency time-varying terms, so the signal average will be

$$\bar{S} = \left[ \frac{1}{2} k_j A^2 - \frac{1}{2N} \sum_{r \neq j} k_r A^2 \right] \left[ 1 - \frac{\sin 2\omega T}{2\omega T} \right], \quad (14)$$

where  $T$  is equal to  $mN\tau$ . It is seen that the last term in the second brackets is  $O(1/T)$  and the signal from the uncorrelated passes is down by a factor of  $1/N$ .

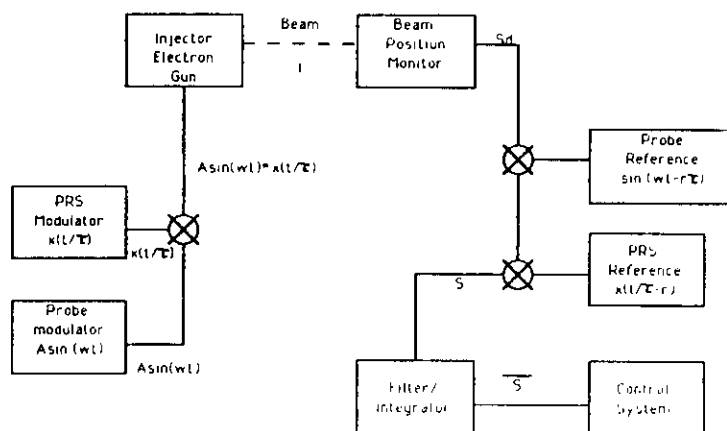


Figure 14. Beam position monitor processing.

A preliminary evaluation of a PRS generator developed at CEBAF has been performed (figure 15). It is a good simulation of the interaction between a beam position monitor and two beam passes, one delayed relative to the other. Our data show the orthogonality characteristic of the PRS autocorrelation function. The results (figures 16-18) show great promise for arriving at a firm design that will be able to distinguish individual beams in the accelerator. In particular, figure 16 shows that two uncorrelated signals have little influence upon one another's signals; this corresponds to two beams' simultaneous signals on one pickup of one beam position monitor. Figure 17 shows the orthogonality of an uncorrelated beam to a particular PRS delay; all uncorrelated PRS delay values show this same resistance to interference. Finally, figure 18 shows the output of the integrator as the PRS sequence is stepped through the entire sequence of delays with both channels at full amplitude. The two correlation peaks are located at the delays at which the PRS sequence is exactly correlated with the two channel sequences.

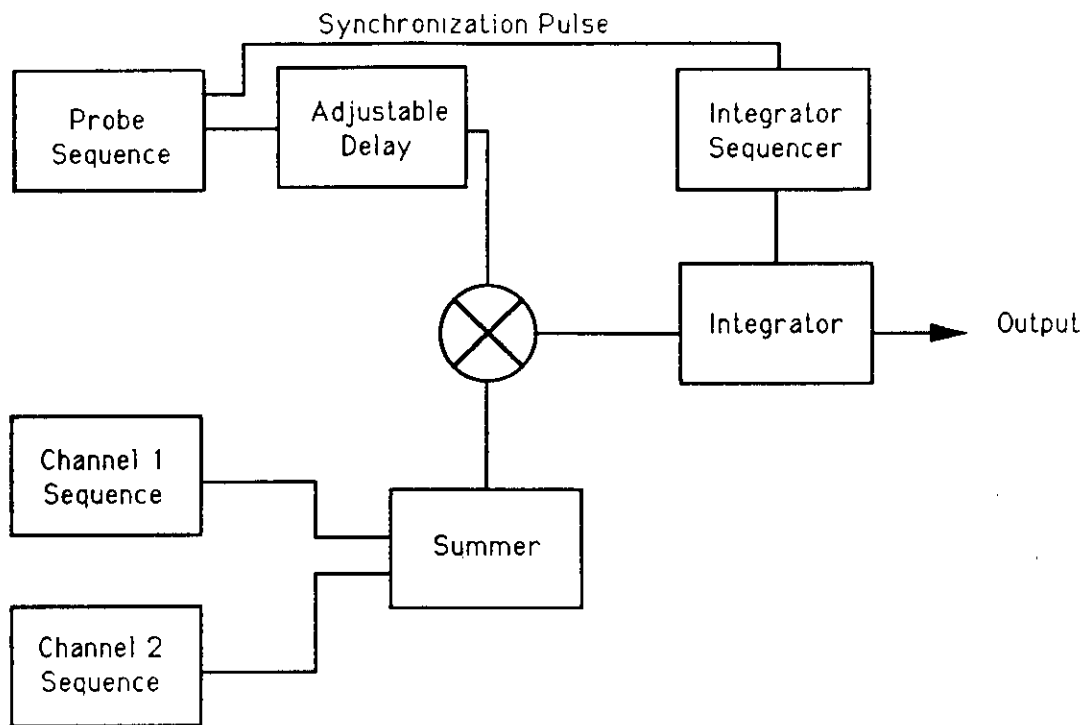


Figure 15. Pseudorandom sequence evaluator.

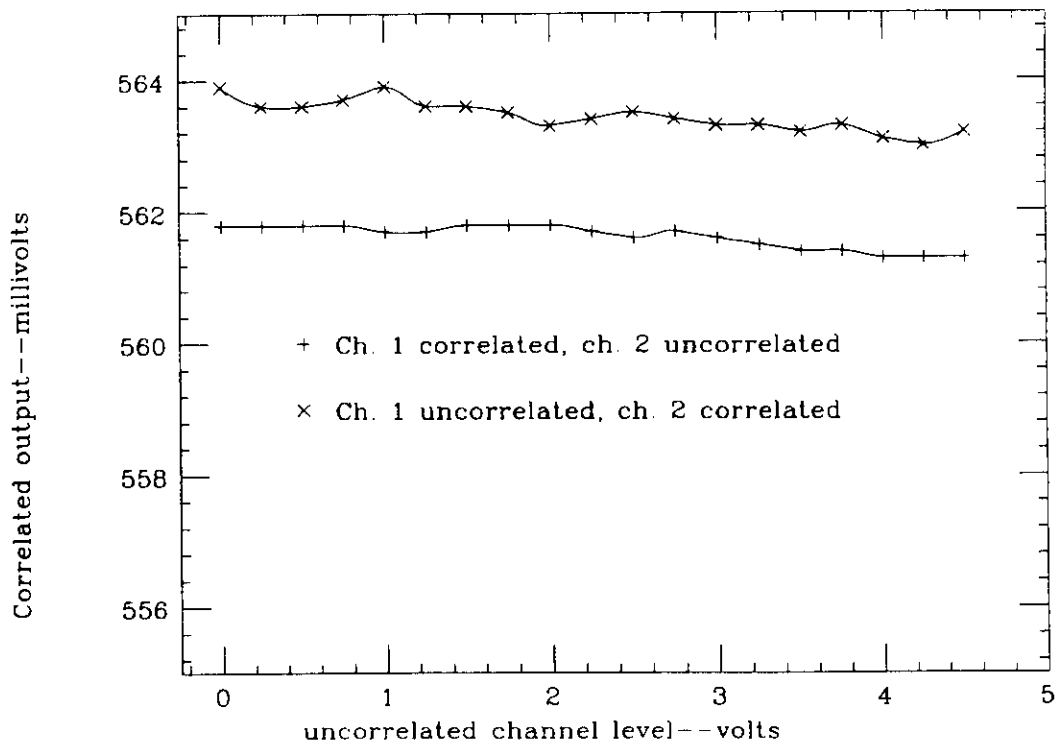


Figure 16. Correlated output vs. uncorrelated signal level.

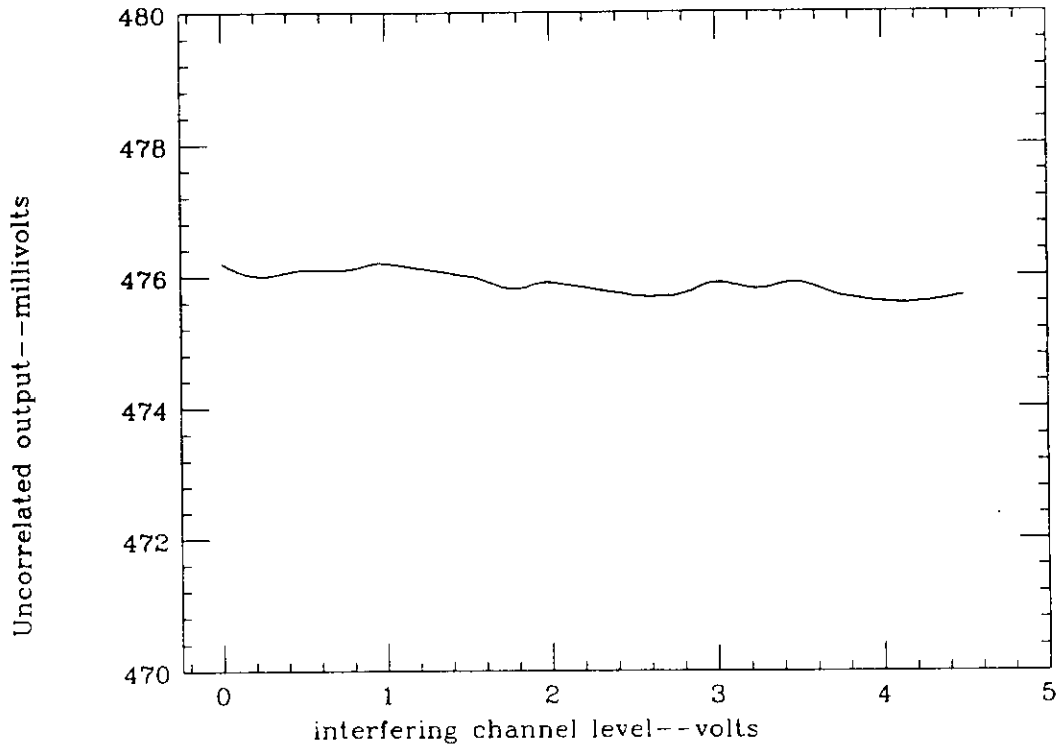


Figure 17. Uncorrelated output vs. interfering signal level.

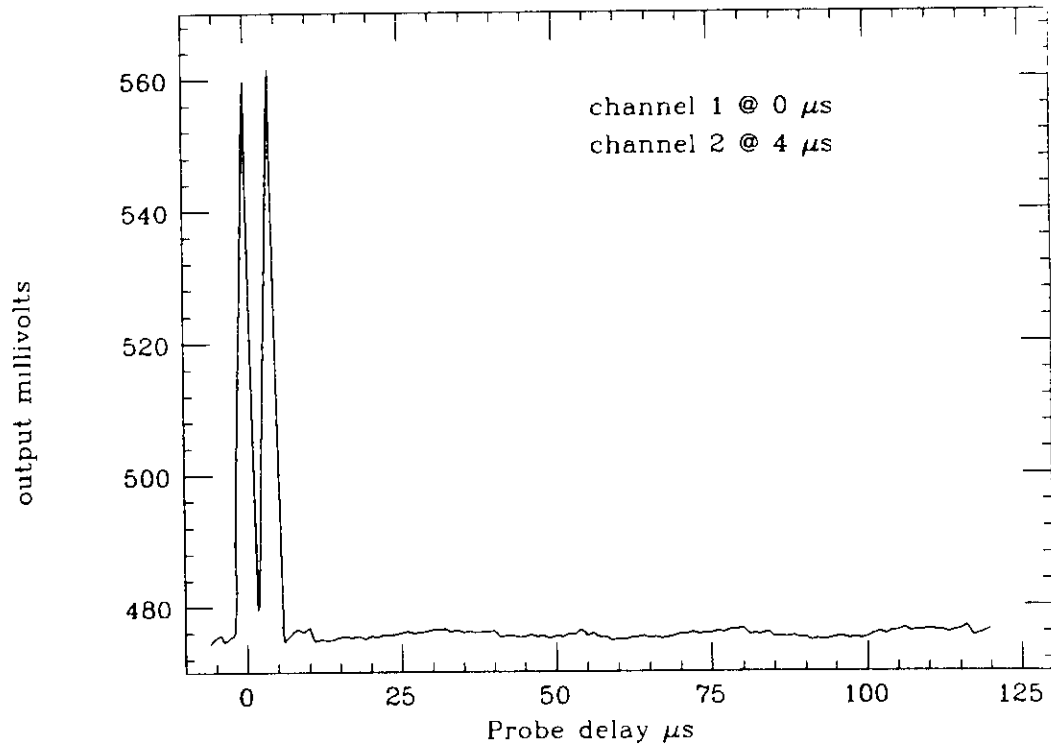


Figure 18. Autocorrelation for two channels.

## IMPLEMENTATION OF PRS AT CEBAF

The pseudorandom sequence BPM system that is described in the previous sections of this paper will be implemented and tested during the CEBAF Front End Tests scheduled to begin in November 1990. A block diagram of the system is shown in figure 19. Comparison with figure 14 will reveal that the actual PRS correlation is performed in software within the microprocessor. There are several advantages to software processing of the PRS:

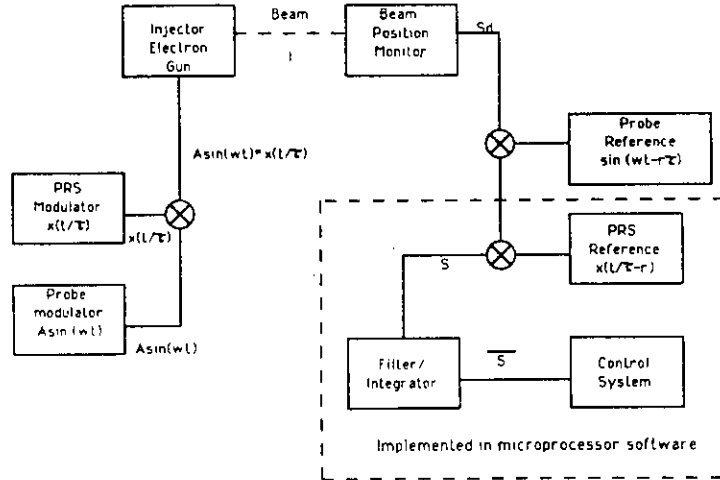


Figure 19. Integration of PRS into existing line receivers.

1. No additional hardware is required over and above that already designed and developed for the CEBAF Linac BPMs.
2. The microprocessor is not subject to the drifts and offsets that are inherent in hardware-based systems.
3. The microprocessor generates the PRS internally and therefore does not require that the sequence be piped around the accelerator, or be generated locally in hardware.

The only changes that will be required in the present system are the reprogramming of the microprocessor to handle PRS correlation instead of signal averaging, reprogramming of the PLDs that control the integrate-and-dump timing, and the addition of a PRS modulator to the injector grid modulation system.

The CEBAF construction schedule does not call for multiple-pass operation of the accelerator for several years. This means that a full functionality test of the PRS BPM system will not be possible during the Front End Test, but multiple-pass operation can be simulated in two ways. The first way is to time shift the PRS modulation at the injector and verify that each BPM must also time shift its internal sequence to locate the beam within the BPM. The second way is to add several time shifted copies of the PRS together prior to the injector grid modulator. Each BPM should then time shift its internal sequence

accordingly and verify that the position of the beam is the same for each of the significant copies of the PRS. Both of these tests are planned for the Front End Test.

## REFERENCES

1. B. Hartline, "CEBAF Progress Report", Proceedings of the 1990 Linear Accelerator Conference, Albuquerque, NM, September 1990.
2. A. Barry, B. Bowling, J. Kewisch and J. Tang, "Orbit Correction Techniques for a Multipass Linac", Proceedings of the 1990 Linear Accelerator Conference, Albuquerque, NM, September 1990.
3. W. Barry, "General Analysis of Thin-Wire Pickups for High Frequency Beam Position Monitors", CEBAF, September 1990 (To be published).
4. W. Barry, "Inductive Megahertz Beam Position Monitors for CEBAF", CEBAF-PR-89-003.
5. A. B. Carlson, Communication Systems, An Introduction to Signals and Noise in Electrical Communication, McGraw-Hill Inc., New York, 1986.
6. W. P. Robins, Phase Noise in Signal Sources, IEE Telecommunications Series, 1982.
7. M. Schwartz, Information, Transmission, Modulation and Noise, McGraw-Hill Inc., New York, 1980.
8. W. C. Barry, J. W. Heefner, G. S. Jones, J. E. Perry, and R. Rossmannith, "Beam Position Measurement in the CEBAF Recirculating Linacs by Use of Pseudorandom Pulse Sequences", Proceedings of the 1990 European Particle Accelerator Conference, Nice, France, June 1990.
9. H. D. Lüke, "Sequences and Arrays with Perfect Periodic Autocorrelation", IEEE Trans. on Aerospace and Electronics Systems, May 1988.
10. S. W. Golomb, Shift Register Sequences, Holden-Day Inc., San Francisco, 1967.
11. G. Krafft and J. Bisognano, "Fluctuations in the Results of Finite Time Averages for Signals of Arbitrary Spectrum", CEBAF TN 90-240.